

Deposition of Single Platinum Nanoparticles on $\text{SrTiO}_3(100)$

A RESEARCH PROJECT AT DESY HAMBURG
SUMMER STUDENT PROGRAMM 2015
21.07.2015 - 10.09.2015



Simon Maier, University of Regensburg

supervised by
Dr. Heshmat Noei and Dr. Thomas F. Keller

Contents

1	Introduction	3
2	The strontium titanate single crystal	3
3	Experimental Part	4
3.1	The molecular beam epitaxy (MBE) chamber	4
3.2	Characterization methods	4
3.3	The Pt evaporator	6
4	Results	8
4.1	Preparation of the SrTiO ₃ (100) Crystal	8
4.2	Pt deposition and posttreatment	9
4.3	Discussion	12
5	Conclusion	14

1 Introduction

To gain a better understanding of platinum nanocatalysis, one can investigate well defined structures, such as epitaxial, small arrays of equidistant Pt nanodots by x-ray diffraction. These arrays can be created by e-beam lithography on strontium titanate (STO) single crystals. An even more simple model systems is a single epitaxial Pt nanoparticle. Since vacuum techniques, e-beam lithography and x-ray focusing are nowadays advanced fields, it is possible to grow the desired particles utilizing molecular beam epitaxy. To find a selected particle with the x-ray beam exploiting the fluorescence signal of hierarchical Pt marker structures deposited in the scanning electron microscopy (SEM) and to focus on this particle with a size between 50nm and 150 nm using for example beamline P10 at PETRA-III with a focus size of $1 \times 1 \mu\text{m}^2$.

The aim of this work was to grow and analyse those single epitaxial Platinum Nanoparticles on $\text{SrTiO}_3(100)$.

2 The strontium titanate single crystal

To grow single epitaxial Platinum Nanoparticles one needs to choose an appropriate substrate, which can be found in SrTiO_3 (STO). STO belongs to the perovskites and its structure is shown in figure 1. The Sr^{2+} and the O^{2-} build a face centered cubic structure with a lattice parameter $a = 0.3905 \text{ nm}$. This matches the fcc structure of platinum with $a = 0.3924 \text{ nm}$. According to Wagner et al. [Wag+01], Pt lies in the region of epitaxial growth on the (100) surface of STO due to the small lattice mismatch $< 0.5 \%$ and a suitable oxygen affinity of Pt.

The STO crystal that was employed in our experiments is a commercial $\text{STO}(100)$ single crystal ($10 \times 10 \times 0.5 \text{ mm}^3$, Crystal GmbH) with a misscut smaller than 0.1° .

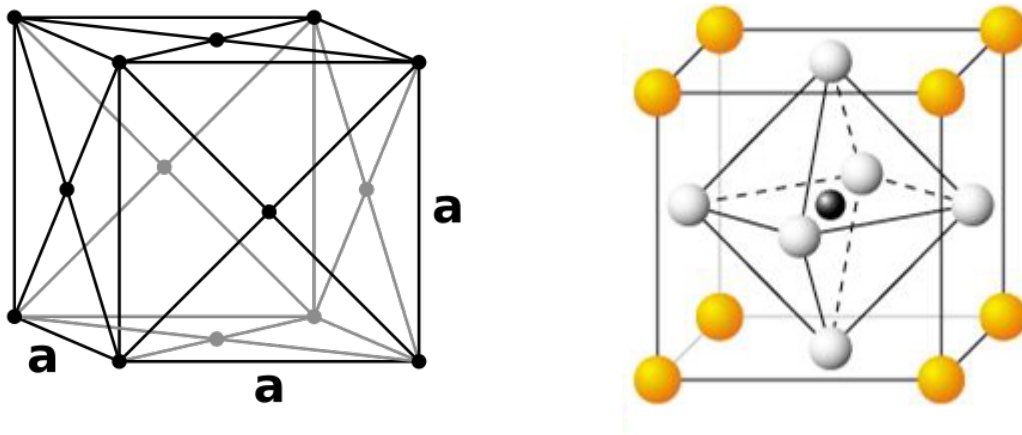


Figure 1: Left [Fcc]: Face centered cubic structure with lattice constant a ; Right [Per]: Perovskite unitcell: In our case the yellow circles represent Sr^{2+} , the white ones O^{2-} and the black circle in the middle stands for the Ti^{4+}

3 Experimental Part

3.1 The molecular beam epitaxy (MBE) chamber

The available ultra high vacuum (UHV) setup consists of several devices: A load lock, an infrared spectrometer (IR), x-ray photoelectron spectroscopy (XPS), an atomic force microscope (STM), a molecular beam epitaxy (MBE) chamber and a tunnel chamber to connect them all. In this work the load lock was used to introduce the sample into the UHV system. After pumping the load lock, the sample was transferred into the MBE chamber via the tunnel, where the deposition procedure took place. A sketch of the MBE chamber is shown in figure 2. The MBE setup is evacuated by a pre-pump, a turbo pump, an ion-getter pump and a titan sublimation pump. Pressures down to 4.9×10^{-11} mbar were reached during the experiments. Once the sample is fixed on the manipulator, one can adjust the spatial coordinates x , y , z and the azimuthal angle φ so that the different devices, that are placed around the chamber, can be faced. In terms of this work only the Pt-evaporator, the low energy electron diffraction system (LEED) and the Auger electron spectrometer (AES) have been employed. The MBE chamber is furthermore equipped with a few more evaporators, a sputter gun and thermal cracker. Additionally one of the sample positions on the manipulator can be heated by a filament and electron bombardment up to approximately 1400 °C (calibration measurement with Al_2O_3).

3.2 Characterization methods

To examine the sample before and after deposition of platinum, several devices have been used. First of all we used surface sensitive methods like low energy electron diffraction

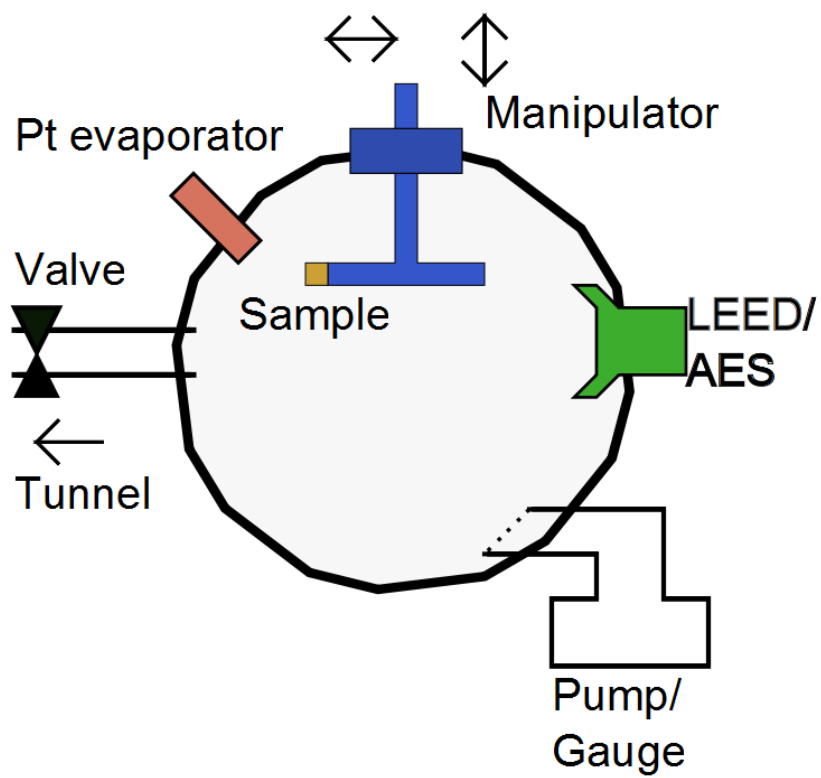


Figure 2: A sketch of the MBE chamber with Pt evaporator, manipulator, LEED/AES system, gauge and pumps, and the valve to the tunnel chamber.

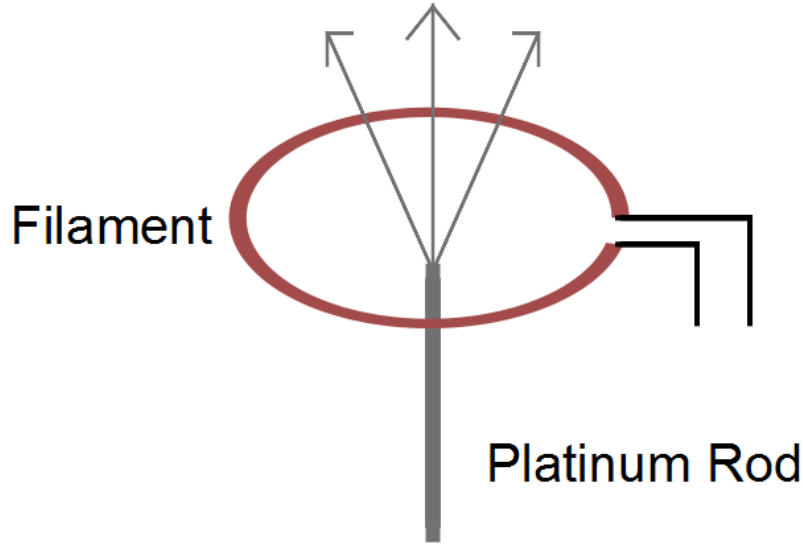


Figure 3: Drawing of the Platinum Rod and the ring filament.

(LEED) and Auger electron spectroscopy (AES) to investigate the composition of the surface. In addition we had a look at the surface after the preparation with atomic force microscopy and recorded a few images with a SEM in several steps of the process, where we also applied energy dispersive spectroscopy (EDS) to get to know the chemical composition of the surface.

3.3 The Pt evaporator

The Pt evaporator is based on electron bombardment to generate intense localized heating. A platinum rod is placed inside a ring filament at ground potential, as it is depicted in figure 3. Electrons from the incandescent filament are accelerated towards the rod due to a high positive potential. Voltages up to 1 kV and emission currents up to 300 mA are achievable [Omi], so that a power of 300 W is delivered into a tiny area, which causes high power densities and thus temperatures from 300 °C up to 3300 °C.

Depending on the material the metal either sublimates, like Iridium, or melts to a little drop, which then evaporates. This is the case for platinum. During the evaporation procedure the rod may be continuously fed into the e-beam heating zone as it evaporates away or the drop falls off. The whole evaporation zone is enclosed by a water-cooled copper shroud with a hole in the direction of the sample. In front of that pocket a flux electrode is installed, which uses a small bias voltage to collect a fraction of the ions that are produced during the evaporation. These ions result in a flux I_{flux} . Because most of the total amount of evaporated material is neutral and not ionized the flux could only be used for calibration, since the number of neutral particles should be proportional to the measured ionized particles. Nevertheless, it is convenient to use the flux to control the stability of the evaporation process.

The geometry of the deposition process is determined by the radius of the hole in

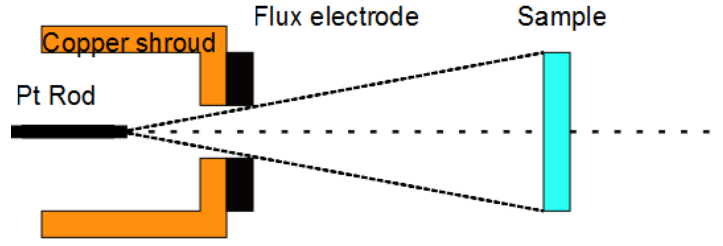


Figure 4: Drawing of the evaporation geometry. To deposit material on the whole sample one needs to put the sample at the right distance.

the copper shroud and the flux electrode. This can be seen in figure 4. Using the rectangular triangle with half of the sample as opposite leg ($d/2$) and the dashed line between the tip of the rod and the middle of the sample as adjacent leg (x), one can apply basic trigonometry to solve this problem. In this case the angle between the adjacent leg and the hypotenuse is called α . This results in:

$$x = \frac{d}{2 \tan(\alpha)}$$

4 Results

In this section the treatment of the STO crystal before deposition of platinum, the deposition process itself and the outcome of the process are described.

4.1 Preparation of the $\text{SrTiO}_3(100)$ Crystal

To gain a clean and single TiO_2 -terminated surface, the strontium titanate crystal was treated as described in [Kos+98]. As the topmost SrO-terminated domains build a strontium hydroxide complex in water, the sample was ultrasonically soaked for 10 minutes in demineralized water. Afterwards the crystal was dipped for about 10 s into a buffered oxide etch with hydrofluoric acid (HF) to dissolve the strontium hydroxide complex. After performing a final annealing step at 950 °C in air for one hour, the sample was examined with atomic force microscopy.

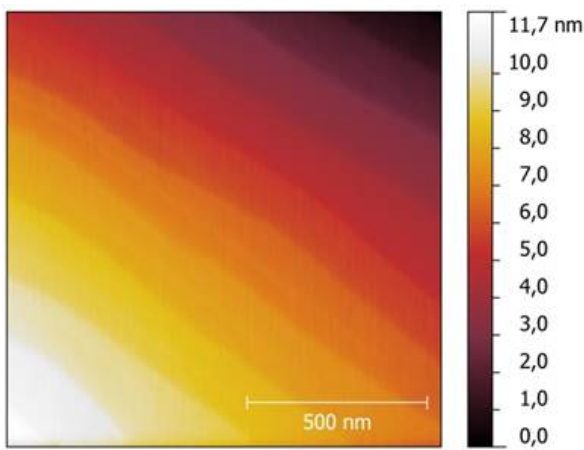


Figure 5: Atomic force micrograph after dipping the STO into buffered oxide etch with hydrofluoric acid and applying 950°C for one hour afterwards.

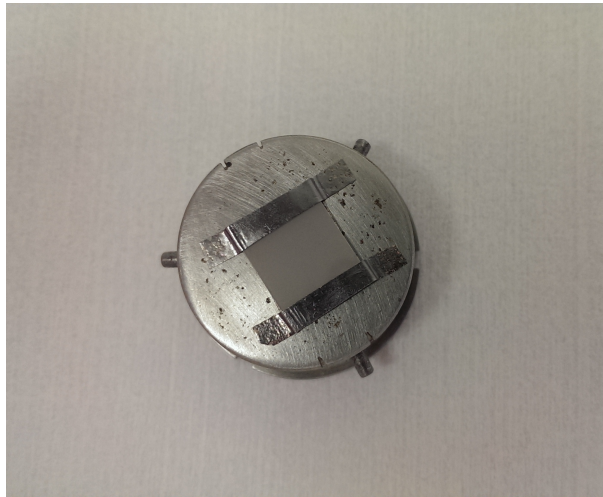


Figure 6: STO sample mounted on a molybdenum sample holder using tantalum clips.

The atomic force micrograph of a sample treated as described above can be seen in figure 5. The sample was mounted on a sample holder as shown in figure 6 to examine it with LEED and AES. The diffraction peaks in the resulting LEED patterns (fig.7) are very clear and symmetrically arranged. Therefore, the crystal structure in the topmost layers seems to be intact and probably not contaminated. This is also confirmed by the black line in the Auger electron spectrum in graph 10, as it shows almost no carbon, which would indicate contamination.



Figure 7: Color inverted LEED patterns of the bare STO at 70eV (left), 100eV (middle) and 170eV (right).

4.2 Pt deposition and posttreatment

A Omicron ERM 3i evaporator was used to deposit the platinum. The filament current was $I_{fil} = 2.14$ A, the emission current $I_{emis} \approx 13.5$ mA and the acceleration voltage $U_{acc} = 1$ kV. An average flux of $I_0 = 4,59$ nA was achieved as it is illustrated in figure 8. Therefore the amount of platinum that has been deposited within $t_{dep} = 416$ min is equal to a single layer with a thickness of $h = 9.7$ Å. During the evaporation process the sample was heated with the temperature $T \approx 800^\circ\text{C}$ to cause dewetting. The pressure decreased constantly from 1.3×10^{-9} mbar at the beginning to 4.5×10^{-10} mbar at the end. The heated sample is depicted in figure 9.

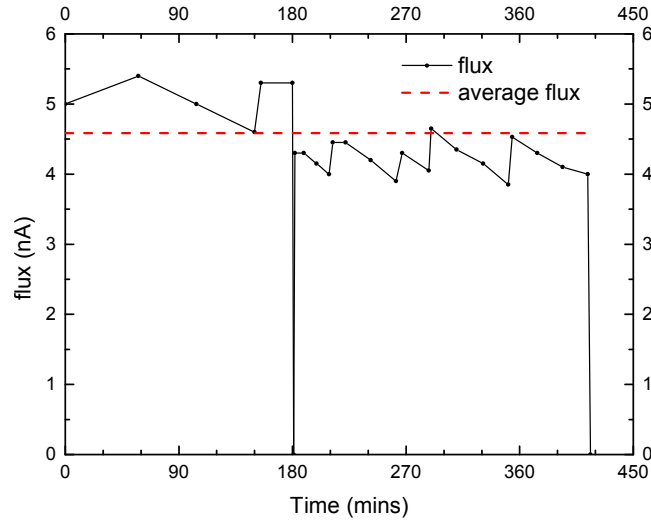


Figure 8: The flux of the platinum evaporator during the deposition process and the average flux.

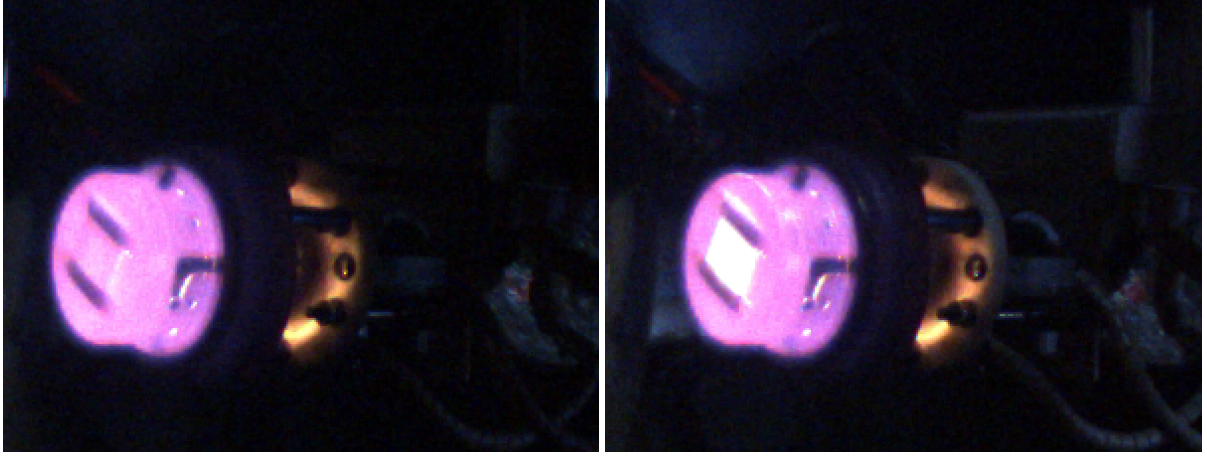


Figure 9: Heating of STO sample in the MBE chamber with and without the spot of the platinum evaporator. The actual color of the glowing sampleholder was orange. ($T \approx 800$ °C)

The AES of the sample after the deposition is demonstrated by the red line in graph 10. Comparing the red line to the black line, only Pt and oxygen peaks can be identified. This leads to the conclusion that almost the whole sample is covered with Pt. This is also confirmed by the SEM measurements we applied (fig.11). Due to charging effects, we could not generate any LEED patterns after deposition.

With the use of the scanning electron micrograph (fig.11), the structures that developed during the platinum evaporation and the heating procedure, can be examined. On the one hand the particles have the desired dimension. The dashed arrows in the third picture point to particles with given diameter of 36.72 nm and 38.03 nm. On the other hand the particles have not separated. Clusters were formed and these agglomerations consist of non equilibrated particles with an undefined shape. One of these is indicated by the black solid arrow. In the second image one can observe a granular structure in between the particle clusters that probably consist of Pt as well. Unfortunately we were not able to apply energy dispersive spectroscopy (EDS) to the best resolution due to charge accumulation.

Due to this outcome, we decided to do one annealing step in air for 10 minutes at 1100°C with a heating rate of 1200 K/h as it was done by Vladimir Komanicky et al. [Kom+09].

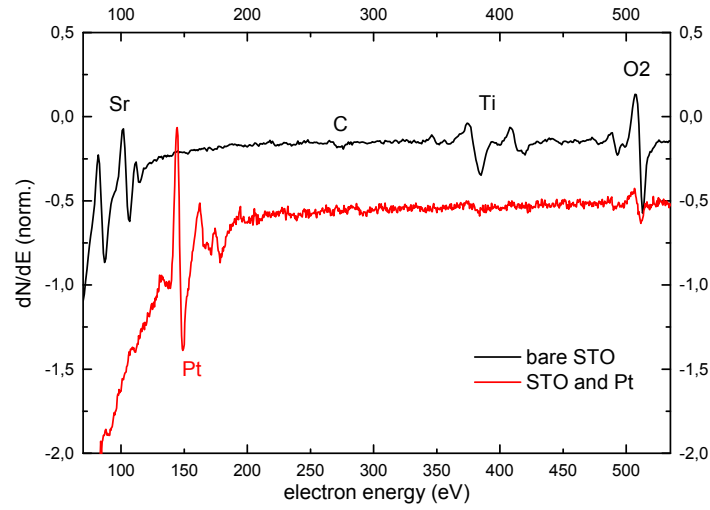


Figure 10: The black line represents the Auger electron spectrum of the bare substrate and the red line the AES of the sample after the deposition of approximately 1 nm Pt. Obviously the bare substrate is very clean.

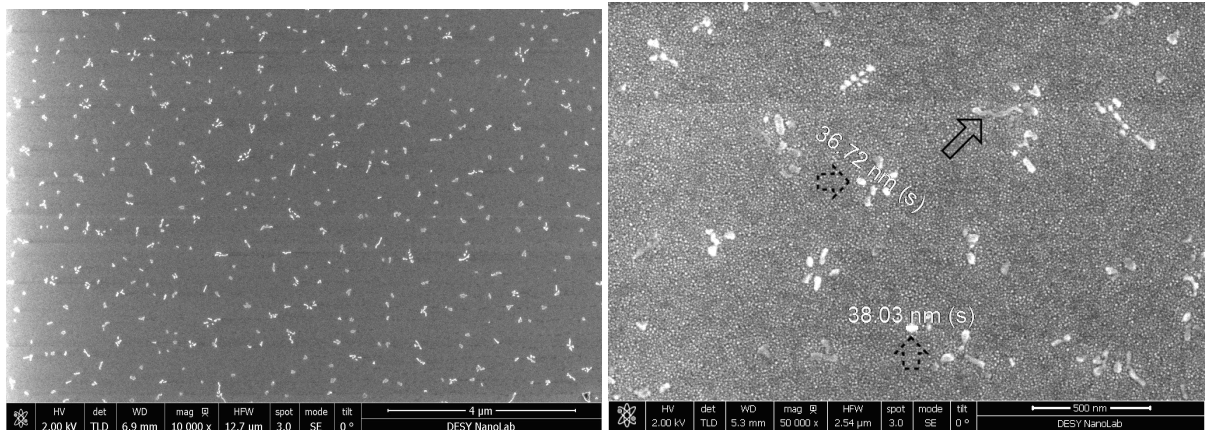


Figure 11: Scanning electron micrographs of the STO crystal after the platinum deposition and before thermal posttreatment. In the second picture one can imagine the granular structure in between the bigger particle.

4.3 Discussion

SEM images of the sample were obtained after final treatments. Having a look at the four images in figure 12 one can state that the particles have equilibrated during the annealing procedure. Especially in the forth frame, four particles with an equilibrated shape can be seen. Furthermore, the size of the particles is distributed, as is the orientation and the density. In the first picture a small particle with 53 nm diameter, a medium one with 74 nm diameter and a large particle with 186 nm are indicated.

Concerning the particle density in the second image, an area of $4 \mu\text{m}^2$ is occupied by 15 Pt crystals. In contrast the third picture only shows one single particle in the same area. This might serve for the proposed beamtime at PETRA III. Since the x-ray beam can be focused down to a size of $1 \times 1 \mu\text{m}^2$, it should be possible to focus on one single particle.[\[SK\]](#)

While analysing the data, one can notice that the particles are orientated in different directions. As the lower edge of the illustrations point towards the $[100]$ direction of the substrate crystal, the particle indicated by the black arrow with the solid outline in the fourth picture is oriented in the $[110]$ direction. Particles that are perpendicular to this one, and therefore turned towards the $[1\bar{1}0]$ direction, can be found in the second frame. The top of the particle, which is indicated by the black dashed arrow, looks like a plateau. This and the form of the particle are hints for epitaxial growth.

Another point that should be mentioned is that the granular structure in between the particle has vanished. In contrast to the sample before the thermal posttreatment, platinum is only measured by an EDS point scan on the particles and not in between them. Several structures between the actual particles can still be discovered, for example in the forth picture indicated by the dashed arrow.

Also the EDS measurement detects no titanium, neither in the particles nor next to them. A likely conclusion would be that the strontium migrates to the surface during the annealing procedure and covers the Ti. However, this does not fully explain the missing Ti peaks, as the Strontium is not expected to segregate over a length scale comparable to the penetration depth of the electrons used for EDS analysis.

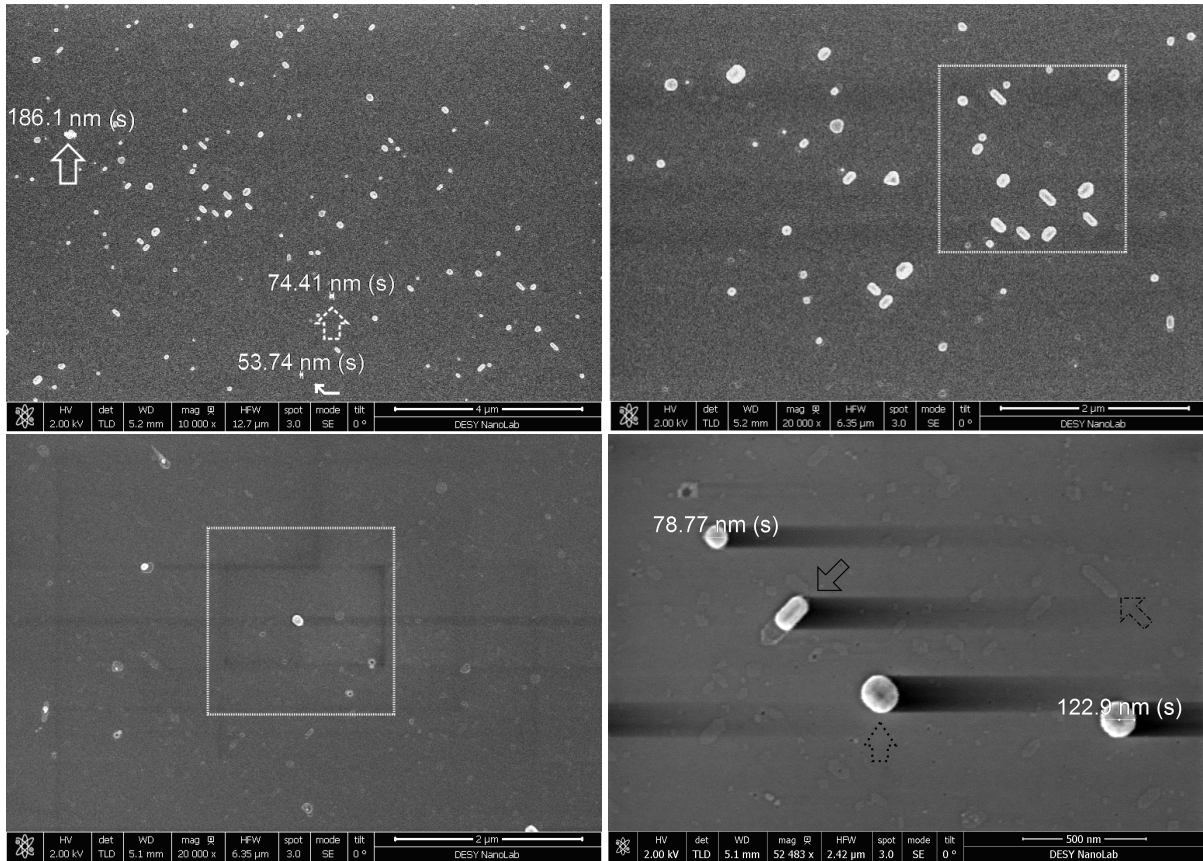


Figure 12: Secondary electron scanning electron micrographs of the STO crystal after the annealing step.

5 Conclusion

The aim of this work was the growth of a single, epitaxial nanoparticle of a catalytically active metal. Therefore platinum on a (100) strontium titanate single crystal was selected. The SrTiO_3 crystal was treated with buffered HF solution to gain a uniform TiO_2 terminated surface. During the deposition of platinum the sample was kept at about 800°C to cause island growth and partial dewetting. A subsequent SEM analysis showed a coexistence of non-equilibrated platinum clusters a granular platinum structure.

To obtain larger and more isolated Platinum nanoparticles, the STO crystal was annealed at 1100°C for 10 minutes. After this, well shaped, more equilibrated single platinum nanoparticles with larger sizes, selected orientations and lower particle surface density were observed by SEM.

Therefore the aim of the project, to grow single platinum nanoparticles, was successfully achieved and the single platinum nanoparticles on STO will likely be examined during a beamtime at the beamline P10 at PETRA III.

Acknowledgement

I appreciate the insight in the daily work with an UHV system that all the members of the research group X-ray physics and Nanoscience of Andreas Stierle gave me. I am extraordinary thankful for their pleasant company and support, in particular to my supervisors Thomas F. Keller and Heshmat Noei who guided me through my research project. Also thanks to Satishkumar Kulkarni, who performed all the SEM measurements. All in all I enjoyed a very informative and educational time.

List of Figures

1	Left [Fcc]: Face centered cubic structure with lattice constant a ; Right [Per]: Perovskite unitcell: In our case the yellow circles represent Sr^{2+} , the white ones O^{2-} and the black circle in the middle stands for the Ti^{4+}	4
2	A sketch of the MBE chamber with Pt evaporator, manipulator, LEED/AES system, gauge and pumps, and the valve to the tunnel chamber.	5
3	Drawing of the Platinum Rod and the ring filament.	6
4	Drawing of the evaporation geometry. To deposit material on the whole sample one needs to put the sample at the right distance.	7
5	Atomic force micrograph after dipping the STO into buffered oxide etch with hydrofluoric acid and applying 950°C for one hour afterwards. . . .	8
6	STO sample mounted on a molybdenum sample holder using tantalum clips.	8
7	Color inverted LEED patterns of the bare STO at 70eV (left), 100eV (middle) and 170eV (right).	9
8	The flux of the platinumum evaporator during the deposition process and the average flux.	9
9	Heating of STO sample in the MBE chamber with and without the spot of the platinum evaporator. The actual color of the glowing sampleholder was orange. ($T \approx 800^\circ\text{C}$)	10
10	The black line represents the Auger electron spectrum of the bare substrate and the red line the AES of the sample after the deposition of approximately 1 nm Pt. Obviously the bare substrate is very clean. . . .	11
11	Scanning electron micrographs of the STO crystal after the platinum deposition and before thermal posttreatment. In the second picture one can imagine the granular structure in between the bigger particle.	11
12	Secondary electron scanning electron micrographs of the STO crystal after the annealing step.	13

References

- [Fcc] Accessed: 8. September 2015. URL: http://chemwiki.ucdavis.edu/%40a%40pi/deki/files/10857/399px-Lattice_face_centered_cubic.svg.png.
- [Per] Accessed: 8. September 2015. URL: http://mrc.iisc.ernet.in/Images/Research_Areas/Original/Image1_Perovskite.jpg.
- [Ati+14] Galit Atiya et al. “Solid-state dewetting of Pt on (100) SrTiO₃”. In: *Mater Science* (2014).
- [HC94] Victor E. Heinrich and P.A. Cox. *The Surface Science of Metal Oxides*. Cambridge University Press, 1994.
- [HG91] Martin Henzler and Wolfgang Göpel. *Oberflächenphysik des Festkörpers*. Vol. 2. Teubner Studienbücher: Physik, 1991.
- [Kom+09] Vladimir Komanicky et al. “Shape-Dependent Activity of Platinum Array Catalyst”. In: *Journal of the American Chemical Society* (2009).
- [Kos+98] Gertjan Koster et al. “Quasi-ideal strontium titanate crystal surfaces through formation of strontium hydroxide”. In: *Applied Physics Letters* 73.20 (1998).
- [Omi] *Omicron Nano Technology, Instruction Manual, UHV Evaporator EFM 2/3/3s/4, Triple Evaporator EFM 3T, IBAD Evaporator EFM 3i*. Limburger Str. 75 D-65232 Taunusstein Germany, 2008.
- [SK] Andreas Stierle and Thomas F. Keller. “Coherent X-ray Diffraction of Epitaxial Pt Nanodot Arrays”. Proposal for a beamtime at PETRA III at DESY Hamburg.
- [Wag+01] T. Wagner et al. “Epitaxial Growth of Metals on (100) SrTiO₃: The Influence of Lattice Mismatch and Reactivity”. In: *Zeitschrift für Metallkunde* (2001).